Journal of Urban and Environmental Engineering, v.11, n.1, p.99-107

ISSN 1982-3932
doi: 10.4090/juee.2017.v11n1.099107

Journal of Urban and Environmental Engineering

www.journal-uee.org

ONE- AND THREE-DIMENSIONAL MODELING OF A VERTICAL-SLOT FISHWAY

Camila Yuri Lira Umeda[1], Guilherme de Lima[2], Johannes Gérson Janzen[1] and Marcio Ricardo Salla[2*]

[1]University Federal of Mato Grosso do Sul, Faculty of Environmental Engineering, Brazil
[2]University Federal of Uberlandia, Faculty of Civil Engineering, Brazil

Received 01 October 2016; received in revised form 02 March 2017; accepted 18 May 2007

Abstract: This paper compares the use of one-dimensional (1-D) and three-dimensional (3-D) numerical models to simulate the flow of a vertical-slot fishway. Prior to their application, the models are validated by comparing the predicted data with experimental data from a physical model. Then the numerical models are applied to calculate four critical hydraulic design parameters of vertical-slot fishways, i.e., flow speed, water depth, turbulent kinetic energy, and energy dissipation rate. Furthermore, the authors developed rating curves for flow rate and energy dissipation rate in terms of flow depth using data from the 1-D model. These curves have great utility for the operation of the vertical-slot fishway studied. The results indicate that 1-D modeling can be a useful tool for preliminary conservative design arrangements of vertical-slot fishways, and that 3-D modeling can be a useful tool to enable accurate representation of the critical hydraulic design parameters and selection of the most appropriate design.

Keywords: Vertical-slot fishway; numerical modeling; computational fluid dynamics; fish passage

INTRODUCTION

Fish of different species migrate within river systems (potamodromy) or between freshwater and marine environments (anadromy) to meet needs (e.g., feeding, reproduction) that cannot be fulfilled otherwise (Bombac *et al.*, 2015; Rodríguez *et al*., 2006). However, the presence of obstructions such as dams interrupts fish migration, reducing the number, biodiversity and distribution of fish populations. In the case of many obstructions, the only way to restore connectivity, at least partly, is to build a fishway (Wang *et al*., 2010).

One of the more common types of fishway designs is the vertical-slot fishway, which consists of a rectangular channel with a sloping floor that is divided by cross-walls into a number of pools forming a linear ladder. Water flows from one pool to the next via a vertical-slot located in the cross-wall. The water flow forms a jet and the energy contained in it is dissipated by circulation and mixing in the downstream pool (Khan, 2006). Fish migrate by swimming from one pool to the next through the slot at any desired depth, using its burst speed. The pools provide an opportunity for resting, till the fish exert burst swimming speed to pass to the next (Rodríguez *et al*., 2006; Clay, 1993).

The effectiveness of a vertical-slot fishway depends on the hydraulic characteristics (e.g., flow speed, water depth, turbulence intensity, and aeration) and biological factors such as the fish's swimming ability, motivation, and behavior (Votapka, 1991). Flow speeds should be less than the sustained swimming capability for each species, and less than burst swimming ability over short distances (Puertas *et al*., 2004; Katopodis, 2012). Additionally, minimum flow depth is required to accommodate fish size, swimming abilities, and behavioral responses (Dane, 1978). Finally, excessive turbulence makes it difficult for the fish to orient themselves correctly, while an abundance of air bubbles can hinder respiration (Rodríguez *et al*., 2006).

Until recently, the hydraulics of vertical-slot fishways was investigated by using physical models (Puertas *et al.,* 2004; Rajaratnam *et al*. 1992; Wu *et al*., 1999). With advances in computer technology and numerical algorithms, computational models are increasingly being used as a convenient and cost-effective means to characterize and predict the hydraulic behavior of vertical-slot fishways. Some researchers have modeled the flow of fishways using one-dimensional and three-dimensional (1-D and 3-D) formulations (Hammerling *et al*., 2016; Marriner *et al*., 2014). However, to our knowledge nobody has used a 1-D model to investigate the flow through a vertical slow fishway and compared the results with 3-D modeling and experimental and/or field data. Applying the 1-D technique to model fishways requires uploading of specified coefficients (e.g., contraction and expansion at the slots) and the introduction of empirical laws to account for recirculation and other phenomena. Additionally, 1-D modeling neglects and highly complex and three-dimensional nature of vertical-slot fishway flows. These flow complexities are captured with 3-D models, which can provide localized flow quantities such as speed, water depth, turbulence kinetic energy, and energy dissipation rate. Nevertheless, 1-D models contain far fewer degrees of freedom and can be executed much faster in comparison to 3-D models, facilitating the obtainment of rating curves (e.g., flow rate in function of flow depth), which have great utility for the operation of vertical-slot fishways.

Therefore, in order to benefit the engineering design of vertical-slot fishways and the further use of 1-D and 3-D models to simulate the hydraulic characteristics of these fishways, the goal of this work is to compare critical hydraulic design parameters (flow speed, water depth, turbulent kinetic energy, and energy dissipation rate) calculated by the 1-D and 3-D models and to develop rating curves for the flow rate and the energy dissipation rate in terms of flow depth using data from the 1-D model. Before their application, the models were validated by comparing the predicted data with the experimental data of a 1:12 physical model developed as part of a real hydroelectric project in Canada.

MATERIALS AND METHODS

Physical model

The computational models were validated using experimental data from a physical model built to 1:12 scale for a hydroelectric project (**Fig. 1**). The fishway is composed of five main parts: (i) entry pool, with width of 5.00 m and length of 5.80 m, located downstream from the dam, at a bottom elevation of 248.00 m; (ii) bypass channel, with bottom at an initial elevation of 251.00 m and width of 3.00 m, composed of 12 pools (numbered from 1 to 12 in Figure 1a); (iii) resting pool with length of 13.70 and bottom at elevation of 253.5 m; (iv) exit pool with length of 4.55 m, which connects the fishway to the reservoir, with bottom at elevation of 255,2 m; (v) water system, consisting of two pipes that discharge an additional flow in the entry pool, to increase the flow and create more attractive conditions for fish to access the fishway without increasing the flow in the bypass channel. The fishway investigated was designed to allow passage of salmon and trout. The pools are connected by slots with height of 2.20 m and width of 0.35 m in baffle walls with a step height of 0.30 m.

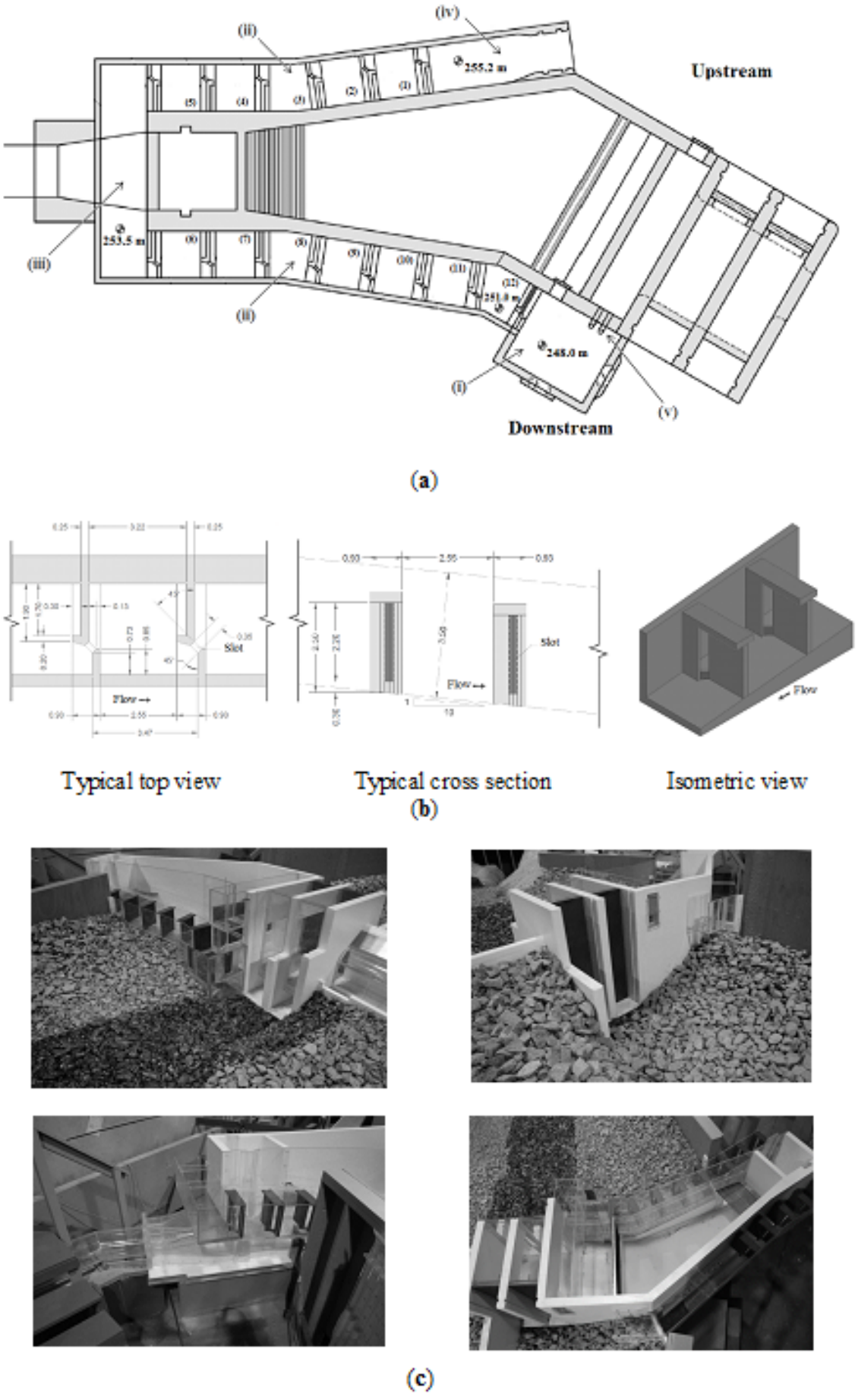

Fig 1 Fishway: (a) identification of the pools and bottom levels in the configuration of the computational model; (b) details of the geometry in the slots in the configuration of the computational model; (c) image of the physical model with 1:12 scale. Source: (NHC, 2013)

One-dimensional flow modeling

The computational modeling was performed using the free program HEC-RAS 4.1 (HEC, 2010), developed by the U.S. Army Corps of Engineers. HEC-RAS uses numerical methods and algorithms to solve a discretized energy equation (Bernoulli equation) for channels in one dimension according **Eq. (1)**.

$$Y_2+Z_2+\frac{\alpha_2 V_2^2}{2g}=Y_1+Z_1+\frac{\alpha_1 V_1^2}{2g}+L\bar{S}_f+C\left|\frac{\alpha_2 V_2^2}{2g}-\frac{\alpha_1 V_1^2}{2g}\right| \quad (1)$$

where: Y_1 and Y_2 are, respectively, the average depths in sections 1 and 2 (m); Z_1 and Z_2 are, respectively, the bottom elevations of the channel in sections 1 and 2 (m) in relation to a reference; V_1 and V_2 are, respectively, the average water velocities in sections 1 and 2 (m/s); α_1 and α_2 are, respectively, the Coriolis coefficients in sections 1 and 2 (dimensionless); g is the gravitational acceleration (m/s^2); L is the length of the reach weighted by the flow (m); S_f is the representative unitary energy head loss of the reach (m/m); and C is the energy head loss coefficient due to contraction or expansion (dimensionless).

The computational procedure of the modeling consists of the following steps (HEC, 2010):

(a) Assume a determined water surface elevation at the upstream cross section ($Y_1 + Z_1$).
(b) Based on the water surface elevation assumed in section 1, determine the corresponding total conveyance (transport capacity of a cross section of the channel) along with the velocity head according **Eq. (2)**.

$$K=\frac{Q}{\sqrt{S_f}}=\frac{1}{n}\times A\times R^{\frac{2}{3}}=\frac{V.A}{\sqrt{S_f}} \quad (2)$$

where: Q is the flow (m^3/s); S_f is the unitary head loss between two sections (m/m); n is the Manning roughness coefficient (m$^{-1/3}$.s); V is the average flow velocity (m/s); A is the hydraulic area of the cross section (m^2); and R is the hydraulic radius (m).

(c) With the values from the previous step, compute S_f and the total head loss between sections 1 and 2;
(d) With the values from the two previous steps, calculate the water surface elevation in the downstream section ($Y_2 + Z_2$) by solving **Eq. (1)**;
(e) Compare the water surface elevation in the downstream section with the value assumed in the upstream section; repeat steps i. to v. until the difference between the water surface elevations is smaller than 0.003 m.

More information about the numerical methods and algorithms used in the tool can be found in the HEC-RAS Hydraulic Reference Manual (HEC, 2010).

With respect to the computational domain of the fishway simulations, some simplifications in the geometry were necessary to adapt it to the 1-D model. The geometry consists of a channel with unique slope (**Fig. 2**), having width of 3.00 m, composed of: (i) an entry pool, with approximate length of 4.38 m; (ii) a bypass channel, composed of 12 pools, each with length of 3.50 m, slots connecting the pools having height of 3.50 m and width of 0.35 m, and a step height of 0.30 m; (iii) a resting pool with length of 14.63 m; and (iv) an exit tank with length of 4.55 m, connecting to the reservoir.

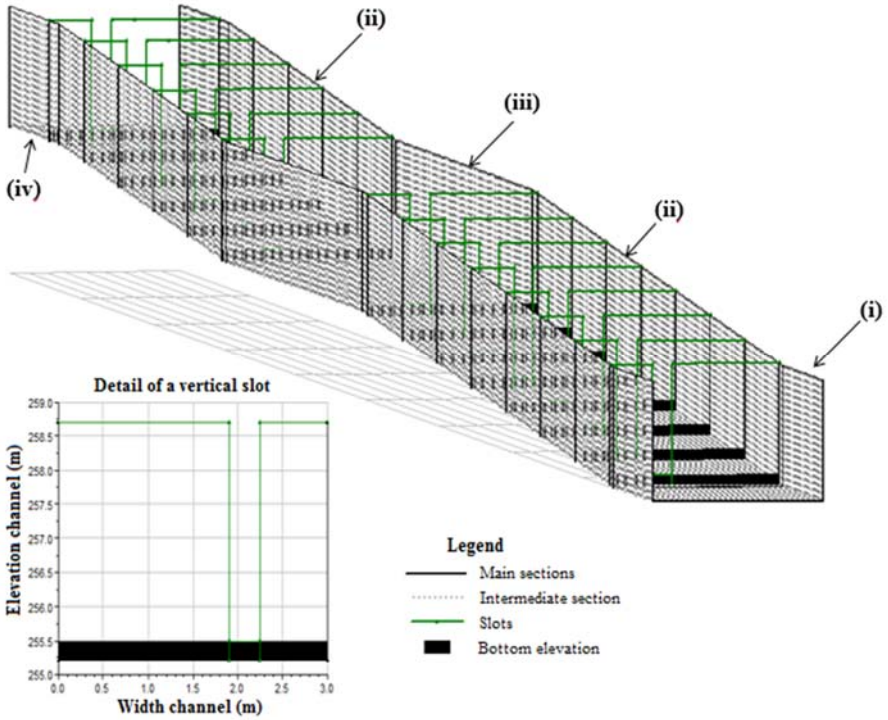

Fig 2 Three-dimensional perspective of the simplified geometry of the fishway, with detail of a cross section with vertical slot.

In the discretization of the cross sections to create the channel geometry, the main sections were added in the regions of cross-sectional narrowing (specifically in the walls with vertical slots) and in the regions where the channel slope changes. Between these main cross sections, intermediate sections were interspersed every 0.10 m, thus creating a more detailed water profile along the fishway. Recirculation regions were placed immediately upstream and downstream from the narrowed section in the walls with vertical slots, considered to be "ineffective" for water transport, where water accumulates. The steps are represented as "obstructions" – areas with blockage to diminish the flow area.

As boundary conditions for the numerical model, the authors used the experimental water levels upstream and downstream from the slots for flows of 1.52, 1.86 and 1.95 m³/s. The Manning coefficient was defined as being constant along the entry channel, equal to 0.013 $m^{-1/3}$.s (Chow, 1973), and the coefficients of contraction and expansion were defined as 0.18 and 0.84, respectively. These values were adopted after the sensitivity analysis and calibration process.

Three-dimensional flow modeling

The 3-D modeling was carried out using the Computational Fluid Dynamics (CFD) technique, by means of the commercial program ANSYS CFX 14.5. This computational code resolves Reynolds-averaged Navier-Stokes (RANS) equations along with conservation and mass equations. Considering a stationary and homogeneous incompressible flow, following **Eqs (3)** and **(4)**.

$$\frac{\partial u_i}{\partial x_i}=0 \quad (3)$$

$$\frac{\partial u_j u_i}{\partial x_j}=-\frac{1}{\varrho}\frac{\partial p}{\partial x_i}+\nu\frac{\partial^2 u_i}{\partial x_i \partial x_j}-\frac{\partial \overline{u_i u_j}}{\partial x_j} \quad (4)$$

In which: i or j is equal to 1, 2, or 3; x_1, x_2, and x_3 denote, respectively, the longitudinal (x), vertical (y) and transversal (z) directions; u_1, u_2, and u_3 are the average velocities in the x, y and z directions, respectively (i.e., $u_1 = u$, $u_2 = v$ and $u_3 = w$); ($u_i'.u_j'$) is the component of the Reynolds stress, where u' denotes the part with fluctuating speed; p is the pressure; and ρ is the specific mass. To calculate the Reynolds stresses, the authors used the Boussinesq approximation, according to **Eq. (5)**.

$$\overline{u_i' u_j'}=\frac{\mu_t}{\rho}\left(\frac{\partial u_i}{\partial x_j}+\frac{\partial u_j}{\partial x_i}\right)-\frac{2}{3}k\delta_{ij} \quad (5)$$

In which: μ_t is the turbulent viscosity; δ_{ij} is the Kronecker delta ($\delta_{ij} = 1$ for $i = j$ and $\delta_{ij} = 0$ for $i \neq j$); and k is the turbulent kinetic energy per mass unit, according to **Eq. (6)**.

$$k=\frac{1}{2}\left(\overline{u_1^2}+\overline{u_2^2}+\overline{u_3^2}\right) \quad (6)$$

Also in the Boussinesq approximation, the turbulent viscosity is calculated from **Eq. (7)**.

$$\mu_t=\rho c_\mu \frac{k^2}{\varepsilon}\,;\ \varepsilon=\frac{k^{\frac{3}{2}}}{L} \quad (7)$$

Where: c_μ is an empirical constant; ε is the energy dissipation rate; L is the length scale; and the distribution of k and ε is calculated from the transport **Eqs (8)** and **(9)**.

$$\frac{\partial \varrho u_j k}{\partial x_j}=\frac{\partial}{\partial x_j}\left(\frac{\mu_t}{\sigma_k}\frac{\partial k}{\partial x_j}\right)+G-\varrho\varepsilon \quad (8)$$

$$\frac{\partial \varrho u_j \varepsilon}{\partial x_j}=\frac{\partial}{\partial x_j}\left(\frac{\mu_t}{\sigma_\varepsilon}\frac{\partial \varepsilon}{\partial x_j}\right)+c_1\frac{\varepsilon}{k}G-\varrho c_2\frac{\varepsilon^2}{k} \quad (9)$$

In **Eqs (8)** and **(9)**, the term G represents the generation of turbulent kinetic energy due to the average velocity gradient, according to **Eq. (10)**.

$$G=\mu_t\left(\frac{\partial u_i}{\partial x_j}+\frac{\partial u_j}{\partial x_i}\right)\frac{\partial u_i}{\partial x_j} \quad (10)$$

The assumed values of the constants were: $c_\mu = 0.09$, $c_1 = 1.44$, $c_2 = 1.92$, $\sigma_k = 1.0$, and $\sigma\varepsilon = 1.3$.

The numerical code uses the finite volume method to solve **Eqs (3)** to **(10)** in three dimensions. In this method, the discretization of the governing equations first occurs by means of spatial division of the domain into various control volumes, which are defined based on a mesh utilizing different schemes. The equations are integrated for each control volume, and the results are used to conserve the relevant quantities such as mass, momentum and energy. The modeling of the free surface (water-air interface) was carried out by the VOF (volume of fluid) method, which solves a set of momentum equations through the domain, maintaining a record of the volume of the two phases in each computational cell. More details about the numerical and computational methods and the theory applied by this program can be found in the CFX® User Guide (ANSYS, 2012).

The 3-D computational domain was created in the CAD (computer aided design) environment, aiming to represent as faithfully as possible the details of the fishway's geometry, with the real dimensions (**Fig. 3**). The arrows in the upper part of the figure indicate the entry flow condition, while the arrows in the lower part indicate the open boundary condition, attributed at the places where the fish access the fishway.

Because of the complexity of the geometry, the authors generated an unstructured mesh, with approximately 10^7 tetrahedral elements. Based on a diagnosis of the mesh quality, which depends on the shape factor of the elements (ratio between an element's

volume and the radius of the circumscribed sphere raised to the third power, where a value of 1 represents a regular element and a value of 0 represents an element with zero volume), the authors verified that 90% of the elements had a shape factor greater than 0.80. The authors refined the mesh further in the regions of the free surface and near the slots (**Fig. 3**), the latter a region having high velocity and water level gradients, to achieve greater detail and better representation of the phenomena that occur there. For the refinement, the authors used an adaptive mesh, i.e., the mesh was refined selectively at the free surface and near the slots according to specific adaptation criteria. This means that while the solution to the problem is calculated, the mesh is refined in places where the variables of the specified solution have larger gradients, with the aim of resolving the flow characteristics in these regions in greater detail.

Specific boundary conditions were defined in the boundaries of the domain (**Fig. 3**). At the outlet of the fishway, the upstream end of the fishway, an entry condition was defined with uniform velocity equal to 0.25 m/s (Q ≈ 1.5 m^3/s). At the access openings to the fishway, the most downstream openings of the fishway, open boundary conditions were defined, allowing the flow to occur in the two directions through the boundary surface. Also, the relative static pressure equal to the hydrostatic pressure, with flow direction normal to the boundary surface, and the fractions in water and air volume were established at these boundaries. The open boundary condition was also applied at the upper limit of the fishway, attributing a relative pressure equal to 0 Pa. The no-slip wall condition was used at the slots, walls and bottom of the fishway. A permanent multi-phase flow condition was assumed (with water and air) in the homogeneous mode for the free surface. The k-ε model was used to describe the turbulence, which uses **Eqs (3)** to **(10)**. This model has previously been used in vertical-slot fishway simulations (Khan, 2006; Marriner *et al*., 2014).

RESULTS AND DISCUSSION

The water depths obtained from the one and three-dimensional models presented close proximity to the water depth of the physical model (**Fig. 4**). The biggest differences between the experimental results and those of the one- and three-dimensional models were 3.3 and 4.1%, respectively, for Q = 1.5 m^3/s. Therefore, the 1-D and 3-D models did a good job of reproducing the water depth and agreed with each other. The greatest difference of the water depth between neighboring pools was 0.44 m, located in the passage of pool 12 to the entry pool. Since step heights of up to 0.5 m are considered satisfactory for passage of the two fish species in question (salmon and trout) (Clay, 1993), the water profile can be considered adequate for their passage.

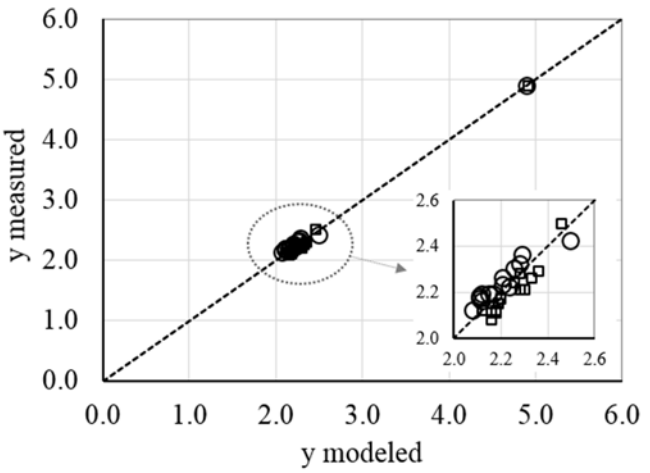

Fig 4 (a) Measured versus modeled water depth for Q = 1.5 m^3/s (□) Three-dimensional model; (○) One-dimensional model.

In an effort to obtain a single ratio between the depth and flow, **Fig. 5(a)** presents the dimensionless depth Y^* (= Y/b) in function of the dimensionless flow Q^* (= $Q/(gS_o b^5)^{1/2}$), obtained from the 1-D model. The profiles fit a single curve very well, indicating the parameters suggested by Rajaratnam *et al.* (1986) for adimensionalization of depth and flow are convergent.

Fish need a minimum water depth to achieve their swimming potential (Dane, 1978), to avoid death due to lack of oxygen, acquire maximum confidence and face low risk of injuries from contact with the fishway bottom. Specific depth requirements vary with species and life

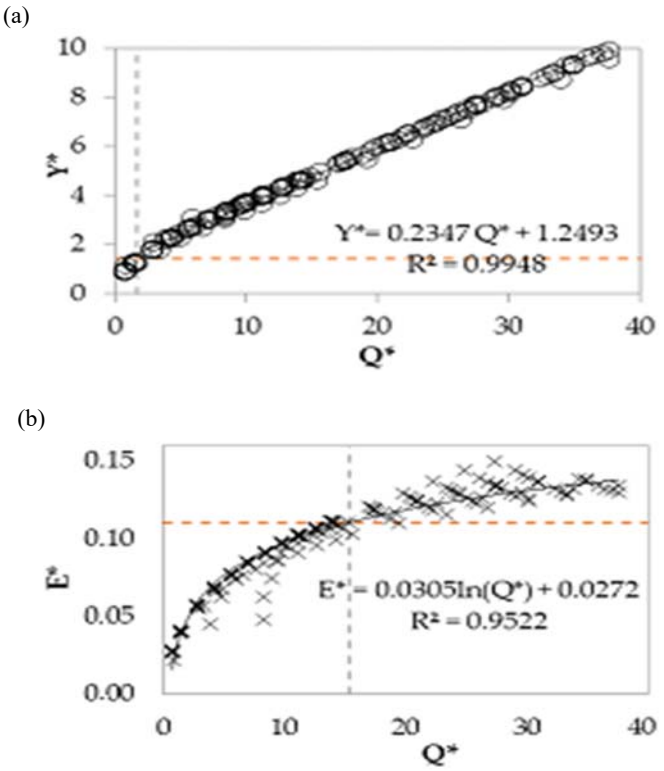

Fig 5 Ratio of dimensionless flow, Q^*, in the fishway pools with (a) dimensionless depth, Y^* (broken lines indicate minimum flow and minimum depth); (b) dimensionless dissipated energy, E^* (broken lines indicate maximum flow and maximum energy dissipation rate). The results presented were obtained from the one-dimensional model.

stage. For salmon, a minimum depth of 0.50 m is usually adopted, while for trout the minimum figure is 0.40 m (Teijeiro *et al*., 2006). Assuming a minimum depth of 0.50 m, the minimum flow to be adopted in the fishway should be approximately equal to 0.12 m³/s.

Figs 6 and **7** present the boundary map of the flow speed along the fishway, with detail of pool 7. Except for the entry, resting and exit pools, the same velocity pattern can be perceived in the pools that form the bypass channel (1 to 7 and 8 to 12). The standard flow in the pools of the bypass channel consists of a high-speed jet flowing through the upstream slot, crossing the pool and colliding with the downstream wall. After this collision with the wall, the flow goes to the downstream slot. On the two sides of the jet there are recirculation regions with low velocities. The recirculation regions provide resting zones for the fish. The intensity of the speed is practically constant as depth increases, except the region located at the slot entry jets, where it increases slightly with increasing depth. The flow pattern found in the pools of the bypass channel is similar to that found by Wu *et al.* (1999) and Liu *et al*. (2006).

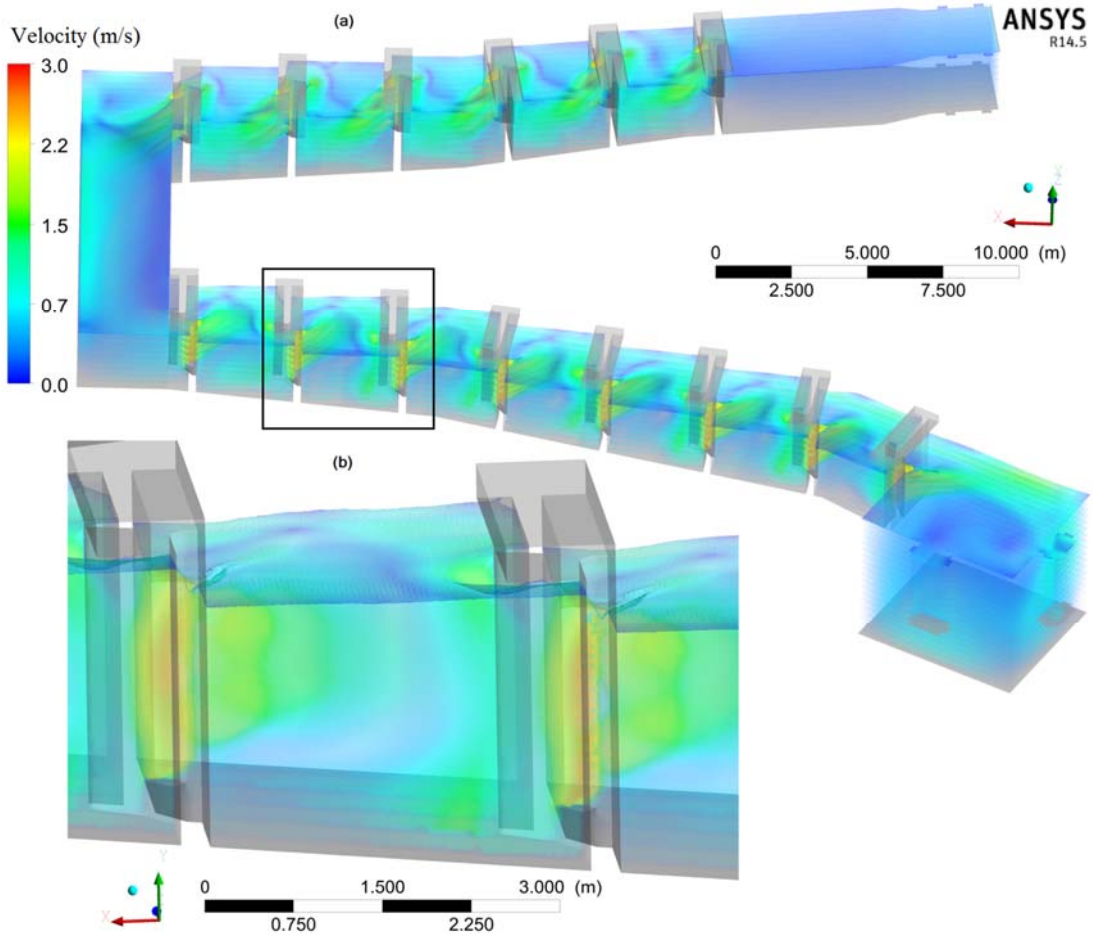

Fig 6 Boundary map of the intensity of flow speed (a) along the fishway and (b) in pool 7.

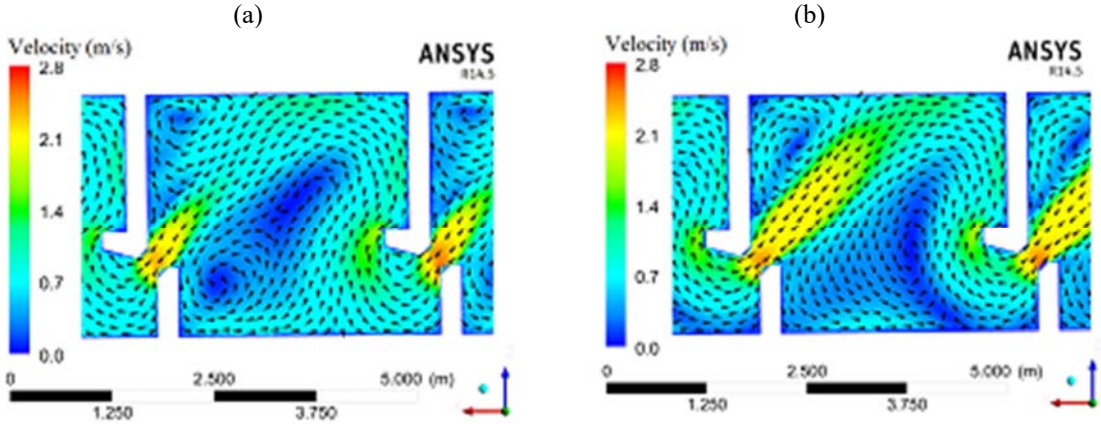

Fig 7 Velocity vectors and boundary map of speed intensity for pool 7 with: (a) $y = 0.25h$; and $y = 0.75h$ (y has origin in the bottom of the pool and points upward).

The fastest speeds (between 1.5 and 2.3 m/s) occur in the slots between the pools and are approximately equal to $(2g\Delta Y)^{0,5}$, where ΔY is the difference in water level between two adjacent pools. For the fish to be able to climb via the pools, the maximum flow should be lower than the maximum burst speed of the fish (Peake *et al.,* 1997). The burst speed of salmon, for example, is 2.7 to 6.2 m/s (Bell, 1991). Therefore, the maximum flow speed is not an impediment considering the burst speed of salmon.

The efficiency of fishways also depends on the turbulence and aeration in the pools. A simple indicator of these parameters is the energy dissipation rate per volume of water, E, calculated from **Eq. (11)**.

$$E=\frac{\rho g Q \Delta Y}{L W Y_m} \qquad (11)$$

where W is the pool width. The higher the energy dissipation value, the harder it is for fish to swim. Substituting Q = 1.5 m³/s and the data for pool 7 in **Eq. (11)** yields a value of E between 200 W/m³ (1-D model) and 240 W/m³ (3-D model). These energy dissipation rates are in good agreement with those obtained in the slots in the 3-D model (**Fig. 8**). However, in the largest part of a typical bypass channel pool, the energy dissipation rate should be lower than 200 W/m³, with an average of 98 W/m³. The lowest average value of E occurred in the resting pool (E = 41 W/m³), while the highest average value was noted in pool 13 (E = 162 W/m³).

Comparison of the values obtained from **Eq. (11)** and the average rates of the three-dimensional simulation (for $y = 0.5h$) shows a difference of 54% in the bypass channel pools, 16% in the resting pool and 41% in pool 13. These results agree with the discrepancies of 8 to 50% found by Liu *et al.* (2006) and Chorda *et al.* (2010). Hence, **Eq. (11)** provides a good estimate of the maximum energy dissipation rate that occurs in the slots, but does not reproduce the values of E found inside the fishway's pools.

To obtain a single curve to describe the ratio between the variables E and Q, the authors removed their dimensions ($E^* = E/(\rho g^{3/2} b^{1/2} \Delta h/L)$ and $Q^* = Q/(gS_o b^5)^{1/2})$) and plotted **Fig. 5b**. Despite a few outliers, the data fit a single curve very well, indicating that the parameters used for adimensionalizing the data are suitable. The literature suggests a maximum E^* value of approximately 0.11 ($E \approx$ 200 W/m³ for the bypass channel pools) for the fishway to allow the passage of fish species like trout and salmon (Rodríguez *et al.*, 2006). In this case the value corresponding to the maximum flow is Q^* = 15.3 ($Q \approx$ 1.10 m³/s). In other words, **Eq. (11)** and the adimensionalization carried out suggest a maximum flow of 1.10 m³/s. These values are

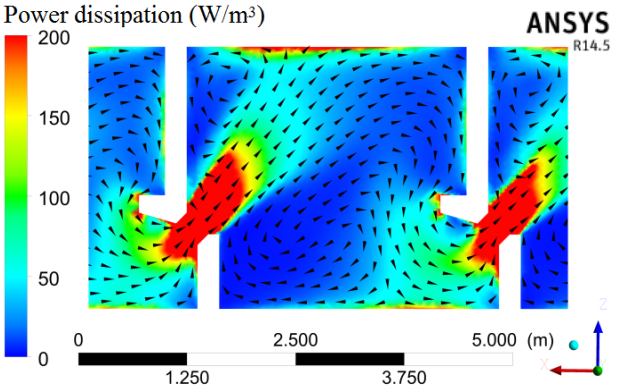

Fig 8 Boundary map of the energy dissipation rate and velocity vectors for $y = 0.5h$ in pool 7.

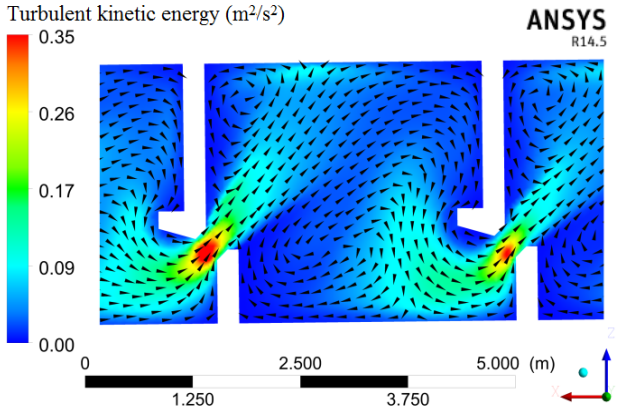

Fig 9 Boundary map of the turbulent kinetic energy and velocity vectors for $y = 0.5h$ in pool 7.

conservative, since the literature indicates that fish can pass through a fishway with much larger values of E and Q using the recirculation regions where the energy dissipation rate is low (Hammerling *et al.*, 2016).

Figure 9 presents boundary maps of the turbulent kinetic energy, k, in pool 7 for $y = 0.5h$. This energy is high (greater than 0.05 m²/s²) in the jet and at the boundary of the recirculation zone, reaching values equal to or greater than 0.35 m²/s². In the recirculation zones, the kinetic energy is high because of the considerable fluctuations in speed as a result of the jet's movement (Enders *et al.*, 2005). In the rest of the pool, the value of k is low (less than or equal to 0.05 m²/s²). The behavior and the k values found in this study are similar to those observed by Liu *et al.* (2006) and Marriner *et al.* (2014). Fish normally tend to avoid strongly turbulent regions, because this reduces their critical speed (maximum speed that a fish can sustain in a current) and increases their energy expenditure (Olla and Davis, 1990; Enders *et al.*, 2003; Enders *et al.*, 2005).

Finally, the passage time through the fishway is negatively correlated with the turbulent kinetic energy (Silva *et al.*, 2012). Hence, high turbulence can impede the passage of fish through the ladder. However, for the simulated flow (Q = 1,5 m³/s), the turbulence does not

appear to be an obstacle for the passage of the two fish species of interest.

CONCLUSIONS

One-dimensional and three-dimensional numerical models were used to simulate the hydraulic behavior of a vertical-slot fishway and the results were compared with data obtained from a physical model. The 1-D model performed well in reproducing the hydraulic characteristics near the slots compared to the physical model, providing conservative information to design these fish ladders, and is considered useful in the initial design phase. The 1-D model also permitted obtaining key curves for flow and energy dissipation rate in function of depth. In turn, the 3-D model not only well reproduced the hydraulic characteristics near the slots, but also those within the pools, enabling a more detailed and accurate evaluation of the hydraulic characteristics along the fishway. Therefore, the 3-D model can be used in the final design phase, during which more detail is necessary than in the initial design phase.

ACKNOWLEDGMENTS The authors wish to thank CAPES for the post-doctoral scholarship provided to the first co-author. The authors also thank Brookfield Renewable Energy for providing information about the physical model and authorizing its use for research purposes.

REFERENCES

ANSYS (2012). *ANSYS CFX-Solver Theory Guide*. Canansburg, PA. Available at: <http://www.ansys.com>

Bell, M.C. (1991). *Fisheries handbook of engineering requirements and biological criteria*. U.S. Army Corps of Engineers, North Pacific Division. Fish Passage Development and Evaluation Program, Third edition.

Bombac, M., Novaka, G., Mlacnik, J., & Cetina, M. (2015). Extensive field measurements of flow in vertical slot fishway as data for validation of numerical simulations. *Ecol. Enging.*, **84**, 476-484.

Chorda, J., Maubourguet, M. M., Roux, H., Larinier, M., Tarrade, L., and David, L. (2010). Two-dimensional free surface flow numerical model for vertical slot fishways. *J. Hydraul. Res.*, **28**(2), 141-151.

Chow, V.T. (1973). *Open-channel hydraulics*. Boston: McGraw-Hill.

Clay, C.H. (1993). Upstream Atlantic Salmon (Salmo salar) Passage. *Proc. Workshop on fish passage at hydroelectric developments,* St. John's, Newfoundland., March 26-28.

Dane, B.G. *Culvert guidelines: recommendations for the design and installation of culverts in British Columbia to avoid conflict with anadromous fish*. Fisheries & Marine Service. Technical Report No. 811. 1978.

Enders, E.C., Boisclair, D., & Roy, A.G. (2005). A model of total swimming costs in turbulent flow for juvenile Atlantic salmon (Salmo salar). *Can. J. Fish. Aquat. Sci.*, **62**, 1079–1089.

Enders, E.C., Boisclair, D., & Roy, A.G. (2003). The effect of turbulence on the cost of swimming for juvenile Atlantic salmon (Salmo salar). *Can. J. Fish. Aquat. Sci.,* **60**, 1149–1160.

Hammerling, M., Walczak, N., Walczak, Z., and Zawadzki, P. (2016). Field and numerical assessment of turning pool hydraulics in a vertical slot fishway. *J. Ecol. Enging*., **17**(2), 81–89.

Hydrologic Engineering Center (HEC) (2010). *River Analysis System, Hydraulic Reference Manual Version 4.1*. U.S. Army Corps of Engineers, Davis, CA. Available at: <http://www.hec.usace.army.mil/software/hec-ras/>.

Katopodis, C. (2012). Ecohydraulic approaches in aquatic ecosystems: Integration of ecological and hydraulic aspects of fish habitat connectivity and Suitability." *Ecol Enging*., **48**, 1-7.

Khan, L.A. (2006). A Three-Dimensional Computational Fluid Dynamics (CFD) Model Analysis of Free Surface Hydrodynamics and Fish Passage Energetics in a Vertical-Slot Fishway. *N. Am. J. Fish. Managm.,* **26**(2), 255-267.

Liu, M., Rajaratnam, N., & Zhu, D.Z. (2006). Mean flow and turbulence structure in vertical slot fishways. *J. Hydrau.l Enging*., **132**(8), 765-777.

Marriner, B.A., Baki, A.B.M., Zhu, D.Z., Thiem, J.D., Cooke, S.J., & Katopodis, C. (2014). Field and numerical assessment of turning pool hydraulics in a vertical slot fishway. *Ecol. Enging*., **63**, 88-101.

Northwest Hydraulic Consultants (NHC) (2013). *Kokish River Hydroelectric Project - Physical Hydraulic Model Study - Final Report*. Knight Piésold Consulting (KP), Canada.

Olla, B.L., and Davis, M.W. (1990). Effects of physical factors on the vertical distribution of larval walleye pollock Theragra chalcogramma under controlled laboratory conditions. *Mar. Ecol. Prog. Ser.*, **63**, 105–112.

Peake, S., Beamish, F.W.H., Mckinley, R.S., Scruton, D.A., & Katopodis, C. (1997) Relating swimming performance of lake sturgeon, Acipenser fulvescens, to fishway design. *Can. J Fish. Aquat. Sci.,* **54**, 1361–1366.

Puertas, J., Pena, L., & Teijeiro, T. (2004). Experimental approach to the hydraulics of vertical slot fishways. *J. Hydraul. Enging.,* **130**(1), 10–23.

Rajaratnam, N., Katopodis, C., & Solanki, S. (1992). New designs for vertical slot fishways. *Can. J. Civil Eng.,* **19**(3), 402–414.

Rajaratnam, N., Van Der Vinne, G., & Katopodis, C. (1986). Hydraulics of vertical slot fishways. *J. Hydraul. Enging.,* **112**(10), 909–927.

Rodríguez, T.T., Agudo, J.P., Mosquera, L.P., and Gonzalez, E.P. (2006). "Evaluating vertical-slot fishway designs in terms of fish swimming capabilities. *Ecol. Enging*., **27**(1), 37–48.

Silva, A., Katopodis, C., Santos, J., Ferreira, M., and Pinheiro, A. (2012). Cyprinid swimming behaviour in response to turbulent flow. *Ecol. Enging*., **44**, 314–328.

Teijeiro, T., Puertas, J., Pena, L., & Pena, E. (2006). Evaluating vertical-slot fishway design in terms of fish swimming capacity. *Ecol. Enging*., **27**, 37–48.

Votapka, F.E. (1991). Considerations for fish passage through culverts. *Transp. Res. Rec*., 1291, 347-353.

Wang, R.W., David, L., and Larinier, M. (2010). Contribution of experimental fluid mechanics to the design of vertical slot fish passes. *Knowl. Manag Aquat Ecosyst*,. **396**(2), 1-21.

Wu, S., Rajaratnam, N., & Katopodis, C. (1999). Structure of flow in vertical slot fishway. *J. Hydraul Eng. ASCE,* **125**(4), 351–360.